European Rotorcraft Forum

HYBRID SOLVER FOR AERODYNAMIC DESIGN

Alexander Nikolsky, anikolskii@gmail.com

Central Aerohydrodynamic Institute named after Professor N. E. Zhukovsky (TsAGI), Russia

Abstract

The low-fidelity generalized inverse solver is developed. It allows to control the pitching moment when the original pressure distribution is corrected. The new hybrid method of aerodynamic design is stated. It uses the generalized inverse solver as a geometry parameterizer along with the solvers of any fidelity to evaluate the objective function

1. INTRODUCTION

It is known that the high-fidelity solvers used in aerodynamic design are very expensive. So the number of iterations has to be reduced to minimum. For this purpose a successful choice of design variables may play an important role. If the designer knows where and how to change the researching geometry of objects the optimization process may be accelerated. The physical considerations help to reduce the number of iterations that is important for expensive 3-d and especially unsteady problems.

The numerical procedures of airfoil design and rotor blade design have many common features.

The airfoil concept is commonly used for surface generation of basic elements of aircraft such as wing, blade, and control surfaces. It is clear that the better airfoil performance the better lifting surface performance. The well known approach for improving airfoil performance is to solve an inverse problem with a given pressure distribution along airfoil surface. But for helicopter airfoils the applications based on inverse problem are limited because of necessity of several flow regimes monitoring simultaneously. So such a way is questionable and not applicable in classical statement. In this study one consider a well posed inverse solver with additional containment providing given pitching moment.

2. INVERSE PPOBLEM WITH MOMENT CONSTRAINT

2.1. Statement

Let in the physical plane z there is an opened contour with semi-infinite cut, flown around by an ideal fluid flow. Let us set the distribution of the pressure coefficient C_p depending on the arc length s counted from the trailing edge of the airfoil in the clockwise direction. Taking into account that for potential flows there is a one-to-one relationship between pressure and velocity modulus u , the velocity distribution can be considered given:$u = f s( )$. It is required to find the contour of the airfoil having a given thickness of the trailing edge, the velocity distribution along which is as close as possible to the given one and at the same time having a given value of the pitching moment at zero lift, C_{m0} . Such a problem we'll name as generalized inverse problem (GIP).

It is known that the solution of the direct problem of the flow around an airfoil with a potential flow of an incompressible fluid is found using a conformal mapping of the outside of the airfoil contour in the z plane to the outside of the circle in the ς' plane. For the convenience of considering the nonlinear case, we add the inversion transformation $\varsigma\,\varsigma=1/'$ to this. Following [1], we represent the derivative of the mapping function in the form:

$$(1)\quad \frac{dz}{} = -\frac{1}{2} \quad - \quad ^{1-\varepsilon} \qquad \sum_{n=0}^{\infty}(1\ \varsigma)$$
$$\exp(\quad c_n\varsigma^n)\ ,\ d\varsigma\ \varsigma$$

where θ is the polar angle in the ς plane, ε is the opening angle of the trailing edge (the angle between the tangents to the upper and lower contours) of the airfoil expressed in fractions of π, $c_n = +a_n \quad ib_n$. In this case, the real and imaginary parts of the logarithm of the derivative of the mapping function can be written as follows:

$$\ln\frac{ds}{} \qquad \sum_{n=0}^{\infty} - -(1\ \varepsilon)\ln 2\sin\theta/\ 2$$
$$= a_n \cos n\theta - b_n \sin n\theta,\ d\theta \qquad \infty\ 1$$

$$\Psi + \frac{1}{2}\left[\theta\ \varepsilon\theta\ \pi + (\ -\ =)\right] \sum a_n \sin n\theta + b_n \cos n\theta .$$

Here Ψ is the angle of inclination of the tangent to the airfoil surface. For potential flows, the velocity modulus in the z plane is related to the velocity modulus in the computational plane ς as follows:

Presented at 46th European Rotorcraft Forum, Moscow, Russia, 8-11 September, 2020

$$\frac{ds}{d\theta} = u(\ )\theta \quad (2)$$

$$u\ s(\ )$$

Once the speed $u(\ )\theta$ is known, solution (2) is reduced to quadratures:

$$(3) \quad \int_0^s u\, ds(\ ) = \int_0^\theta u\, d(\ )\theta\theta$$

By integrating this relationship, we obtain the dependences $s(\ )\theta$, $\Psi(\ )\theta$ and determine the coordinates of the airfoil contour $x(\ )\theta$ и $y(\ )\theta$:

$$(4) \quad x(\theta) = \int_0^\theta \frac{d\theta}{ds} \cos(\Psi) d\theta\ ,\ y(\theta) = \int_0^\theta \frac{d\theta}{ds} \sin(\Psi) d\theta$$

It remains to find out what conditions the function $H = \frac{ds}{d\theta}$ must satisfy in order for the solution to exist, the airfoil obtained as had a given thickness of the trailing edge, and its pitching moment at zero lift had a given value. By integrating relation (1) and using the theory of residues, we obtain the function H constraints to provide the conservation of the velocity at infinity and a given thickness of the trailing edge:

$$\int_0^{2\pi} \ln H d\theta = 0\ ,$$

$$\int_0^{2\pi} \ln H \sin(\theta) d\theta = 0,$$

$$(5) \quad \int_0^{2\pi} \ln H \cos(\theta) d\theta = c_{11} .$$

Δy^{te} Δy_{te} is the thickness of the

Here $c_{11} = -\ -(1\ \varepsilon)\ ,\ 2\pi$

trailing edge referred to the airfoil chord. From the Chaplygin - Blasius formula one obtain an additional H constraint to provide the given value of the pitching moment at zero lift:

$$(6) \quad \int_0^{2\pi} \ln H \sin(2\theta) d\theta = -\frac{C_{m0}}{4} .$$

These integral relations, as well as the Lighthill relations, do not allow modifying the target velocity distribution in advance before solving the problem, since it requires knowing the $s(\ )\theta$ dependency . However, conditions (5), (6) have the advantage in that they are applicable to the nonlinear case, and a simple way to satisfy them is indicated below. For this, as in [2], we define H_m in the following form:

$$(7) \quad H_m = H \exp g .$$

Here and below, the index m denotes a modified function. We will seek a function H_m close to a given function H in the sense of least squares that satisfies integral relations (5), (6). Let us rewrite these relations for the function g:

$$\int_{\theta_1}^{\theta_2} g d\theta = -\int_0^{2\pi} \ln H d\theta = -a_0 2\pi$$

$$\int_{\theta_1}^{\theta_2} g \cos\theta d\theta = -\int_0^{2\pi} \ln H \cos\theta d\theta = -(a_1 - c_{11})\pi$$

$$\int_{\theta_1}^{\theta_2} g \sin\theta d\theta = -\int_0^{2\pi} \ln H \sin\theta d\theta = -b_1 \pi$$

$$(8) \quad \int_{\theta_1}^{\theta_2} g \sin 2\theta d\theta = -\int_0^{2\pi} \ln H \sin 2\theta d\theta = -(b_2 + \frac{C_{m0}}{4})\pi .$$

It is seen that for the case when the function H , and with it the target velocity u , is modified over the entire surface of the airfoil, which corresponds to the range $0 \le \le \theta\ \pi 2$, there is an exact solution to the system of equations exist :

$$g = -\ -\ -a_0 \qquad (a_1\ \ c_{11})\cos\theta - b_1 \sin\theta -$$

$$\frac{C_{m0}}{4} \quad (9) \quad -\ +(b_2 \qquad)\sin 2\theta .$$

This solution differs from the solution for the classical inverse problem [2] by an additional last term on the right-hand side of relation (9). Now, substituting (9) into (7), one determine H_m , and hence Ψ_m . Then, from

Presented at 46th European Rotorcraft Forum, Moscow, Russia, 9-11 September, 2020

relations (4), we find the coordinates of the desired airfoil in a parametric form. In contrast to the direct problem, in the inverse problem the angle of attack is not known in advance, but is determined from the relation $\alpha\ \gamma = f(\ )$. Here $\gamma = \frac{\Gamma}{\Gamma_{min}}$, Γ_{min} is the velocity circulation along a part of the airfoil contour from the trailing edge to the front stagnation point along the lower surface of the airfoil, Γ is the total circulation:

$$\Gamma_{min} = \int_0^{\theta_0} u(\theta)d\theta\ ,\ \Gamma = \int_0^{2\pi} u(\theta)d\theta\ .$$

For an incompressible fluid, the dependence of the velocity on the angle of attack is known: $u(\ )\theta = -2[\sin(\theta\ \alpha\ \alpha +\ +)\ \sin\ ]$, $\theta\ \pi\ \alpha_0 = -2$. After performing the integration, we obtain the following equation to determine α: $tg\alpha = \frac{\gamma}{[\pi\gamma/2 - 1 - \alpha\gamma]}$

This means that for the case of an incompressible fluid, the solution to the GIP is obtained in quadratures.

In the nonlinear case, the solution and the angle of attack are obtained at the current iteration, which will be discussed below. Of greatest interest is the solution holding the pressure distribution of the pressure distribution over the upper surface of the airfoil, which determines the level of the maximum lift coefficient C_{Lmax}. In this case, the modification is performed along the low surface of the airfoil, and the solution is not universal. Let's set the modification range as $\theta\ \theta\ \theta_1 \le\ \le\ _2$, denote $\varphi = \frac{(\theta - \theta_1)}{2\pi}$, $0 \le \varphi \le 2\pi$. As in [2], we represent the function g in the form of a finite Fourier series:

$$(10)\quad g = \sum_{n=0}^{N} d_n \cos n\phi + e_n \sin n\phi.$$

At the ends of the modification interval, we impose the smooth conjugation conditions: $g(0) = g(2\ )\pi = 0$, $g'(0) = g'(2\ )\pi = 0$. The least squares method is reduced to finding the minimum of the functional:

$$\int_{\theta_1}^{\theta_2} g^2 d\theta + \lambda_1 g(0) + \lambda_2 g'(0) + \lambda_3 (\int_{\theta_1}^{\theta_2} g \sin\theta d\theta + b_1\pi) +$$

$$+\lambda_4 [\int_{\theta_1}^{\theta_2} g\cos\theta d\theta + (a_1 - c_{11})/\pi] +$$

$$+\lambda_5 [\int_{\theta_1}^{\theta_2} g \sin 2\theta d\theta + (b_2 + \frac{C_{m0}}{4})] = \min\ \_\_\_\_\ .$$

Solving the system of equations of 5-th order, we find the modifying function g, and hence the functions H_m and Ψ_m. Again, using formulas (4), we obtain a solution to the GIP for an incompressible fluid. At the same time, the target velocity distribution over the upper surface of the airfoil is provided.

For a nonlinear problem, when the velocity $u(\ )\theta$ in the computational plane in equation (2) is not known, as in [2], we will solve the GIP by the method of successive approximations.

Assuming the function $s(\ )\theta$ to be known at the k-th iteration, we solve the direct problem for the full potential equations (FPE) and find the velocity $u_k(\ )\theta$. ds^{k+1} $u^k(\ )\theta$

Equation (2) will take the form: = .

$d\theta\ u\ s(\ )$

By integrating it, we find the next intermediate approximation s_{k+1}, solve the system of equations and determine g_k. We find the following approximation that satisfies conditions (8):

$\overline{ds_{k+1}} = \overline{ds_{k+1}} \exp g_k$. And so on until the $d\theta\ d\theta$

$\left|\overline{ds^{k+1}} - \overline{ds^k}\right| < \delta$ is reached, convergence criterion

$d\theta\ \theta d$

where δ is a small parameter. During iterations when solving the direct problem, it is not the value of the angle of attack that is set, but the value of the

Γ parameter $\gamma = \frac{\Gamma}{\Gamma_{min}}$, and the angle of attack is determined in the process of solving from the KuttaZhukovsky condition.

2.2. Application

Consider the application of GIP to the design of helicopter airfoils. In the aerodynamic design of helicopter airfoils, the restrictions are usually imposed on the airfoils C_{m0} value. For the sake of

Presented at 46th European Rotorcraft Forum, Moscow, Russia, 9-11 September, 2020

clarity, let's assume that it is necessary to change C_{m0} value towards the pitch up.

This increase of C_{m0} for helicopter airfoils is usually achieved changing angular tab position upward. This, in turn, leads to a decrease in the values of C_{Lmax}. In our case, the GIP is solved holding the pressure distribution over the upper surface. Since, in the first approximation, the target C_L is also preserved

(exactly for $M_\infty = 0$), one should expect that C_{Lmax} of the modified and original airfoils will be close.

Consider NACA-23012 airfoil with the trailing edge tab installed along its chord. Target pressure distribution is calculated by the direct FPE method at near C_{Lmax} flow condition: M_∞ =0.4, C_L =1.4. The GIP problem is solved provided that the original airfoil C_{m0} is increased by 0.01. Let us designate the airfoils as follows: obtained as a result of the GIP solution - N230m, original airfoil - N230, original airfoil with tab deflected by 2 degrees upwards - N230up.

Figure. 1 shows the C_p distributions and contours of the airfoils.

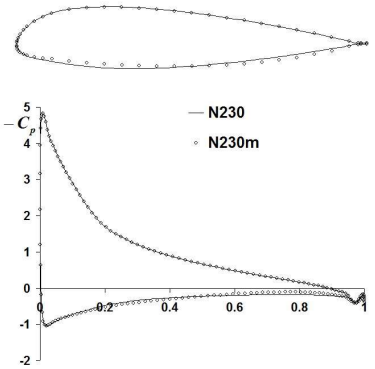

Figure 1. Airfoils contours and pressure distributions. M_∞ =0.4, C_L =1.4

The coefficients of the pitching moment C_{m0} and maximum lift C_{Lmax} of the airfoils were calculated using the CFD RANS solver. Compared with the original airfoil, the following increments were obtained: ΔC_{m0} = 0.0119, ΔC_{Lmax} = -0.0048 for the

N230m airfoil and ΔC_{m0} = 0.0088, ΔC_{Lmax} = -0.021 for the N230up airfoil. The calculated data confirm the above stated advantage of the N230m airfoil obtained as a result of the GIP solution over the N230up airfoil obtained as a result of the upward deflection of the tab. Thus GIP method allows for modifying the lower surface of the airfoil, which makes it possible to increase the pitching moment of the airfoil without a noticeable decrease in its maximum lifting capacity. This allows the method to be used in aerodynamic design of airfoils, in particular for helicopter blades.

3. COMBINED AERODYNAMIC DESIGN METHOD

The problem of aerodynamic design of helicopter airfoils is multi-criteria one, since it is necessary to provide favorable airfoil performance for at least three main flow conditions. The attractiveness of aerodynamic design of airfoils by the method of solving the inverse problem is due to the fact that, in contrast to methods using a direct solver and enumeration of numerous iterations in the GIP method, the type of target distribution is set by the user based on physical considerations. However, when the target pressure distribution is achieved in one design flow conditions, there is no control over the performance in other basic flow conditions, therefore, to implement such control, it is necessary to involve a direct solver. We use the following considerations to define such a procedure. On the upper contour of the airfoil, three regions (along arc length s) can be conditionally distinguished, shown in Figure 2, which have the great effect on the values of the main integral criteria: maximum lift coefficient $C_{L\max}$, maximum aerodynamic efficiency $K_{\max}$ equal to lift to drag ratio $(L/D)_{\max}$ and drag near divergence Mach number M_{dd}.

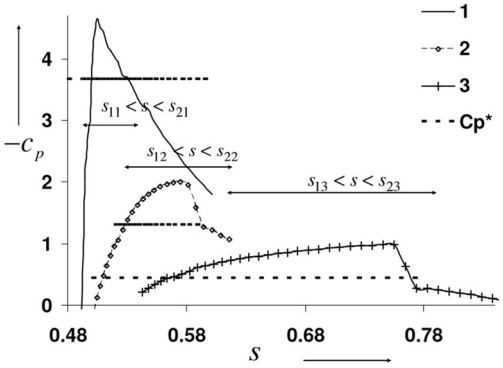

Figure 2. C_p distributions and three main regions and flow coditions:

1- M_∞ =0.4, $C_L \approx C_{Lmax}$, 2-M_∞ =0.6, $C_L \approx 0.6$,

3-$M_\infty \approx M_{DD\infty}$, C_L =0. C_{p^*} - Critical value

Analysis of the numerical and experimental data shows that, with near fixed pressure distributions in

Presented at 46th European Rotorcraft Forum, Moscow, Russia, 9-11 September, 2020

the diffuser part of the airfoil, the $C_{L\max}$ value is mainly defined by the size and shape of the nose pressure peak. Therefore, near the leading edge of the airfoil, there is a local region $s_{11} < < s\ s_{21}$ that determines the magnitude of the pressure peak and the character of flow deceleration in the supersonic flow region, which has a decisive effect on the $C_{L\max}$ value. In the adjacent region $s_{12} < < s\ s_{22}$ in the vicinity of the $K_{\max}$ flow condition a supersonic zone is formed, which has a decisive effect on the magnitude of the wave drag. Suppose that a suitable local correction of C_p can be used for reducing the wave drag. If the flow in this region is mainly subsonic, the drag value is determined by the value of the frictional drag, and the correction must be selected from another considerations. An extended region $s_{13} < < s\ s_{23}$ that follows the second region, in which a shock is formed at transonic flow conditions, in which the correction must be selected in such a way as to slow down the growth rate of the wave drag. Numerical experiments were carried out and show that:

the value of the maximum lift of the airfoil can, generally, be increased without a noticeable reducing of the other two criteria due to a local change in the pressure coefficient in the vicinity of its peak; the value of the maximum aerodynamic quality of the airfoil can, generally speaking, be increased without a noticeable deterioration reducing of the other two criteria due to a suitable change in the pressure coefficient in the supersonic zone; the wave drag of the airfoil can, generally , be increased without a noticeable deterioration reducing of the other two criteria due to a suitable change in the pressure coefficient in the supersonic zone.

Of course these statements are valid if the airfoil shape is not completely optimized according to the considered criteria and are clear from the physical considerations. The problem consists in finding the boundaries of regions and suitable choice of C_p in these regions.

Thus the combined aerodynamic design method is based on the following considerations: the method for solving the GIP allows in the near vicinity of the original airfoil contour to form a family of airfoil contours having a fixed C_{m0} value and differing locally by C_p distributions; the method for solving the direct problem allows to determine the airfoils performances, and the optimizer to choose the optimal airfoil contour. Scheme of design is presented in Figure 3

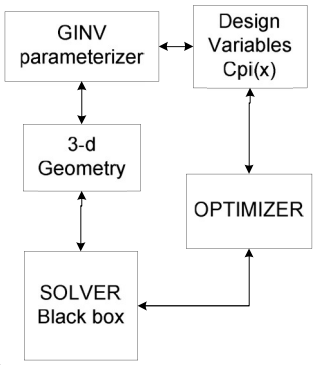

Figure 3. Scheme of design

The approach considered is applicable to the solvers of any fidelity (3-d, unsteady). The only limitation is airfoil based geometry, for example blade and wing surface. The purpose of the present study was to clarify the applicability of this mathematical model to successive improvements of integral aerodynamic criteria for helicopter airfoils. Based on the method of solving of GIP, the procedure is developed for pressure distribution control on typical flow conditions for successive improvements of helicopter airfoil performances. The design procedure consists of three successive optimization cycles at the main flow conditions around helicopter airfoils, each of which consists in finding the optimum of the objective function: $G\ X_j(\ ) = \lambda_{1j}(C_{Lmax0} - C\ X_{Lmax}(\ )) + \lambda_{2j}(K_{max0} - K\ X_{max}(\ )) + \lambda_{3j}(C_{D0} - C_{D0\,0}(\ ))X$, j = 1,2,3.

Here X is the vector, the components of which are arc abscissas of the control points, and the boundary points themselves and the pressure coefficients at these points, Subscript 0 denotes target values, C_{d00} - drag coefficient near M_{dd} flow condition, N_j is the number of control points. The weight functions λ are set in such a way as to satisfy the aerodynamic constraints with sufficient accuracy. The number of design parameters in j -th cycle is equal to $N_j + 2$ because the location of the boundary points is not known in advance. Since the arc abscissas of the first and last control points were design variables, in the process of solving such a range was automatically set, in which the correction did not lead to a reducing of the remaining integral criteria. In this case, in each of the optimization cycles, by choosing the appropriate weight functions (established in the numerical experiment), the levels of two of the main criteria were fixed, and the third was optimized.

The airfoil contour is determined from the solution of the inverse problem, and the main integral aerodynamic characteristics included in the objective function are calculated using a direct solver. The problem was solved in two versions based on solvers of different fidelity levels viscid-invicid, VISTRAN [3]

Presented at 46th European Rotorcraft Forum, Moscow, Russia, 9-11 September, 2020

and CFD RANS [4]. This was done in order to define the possibility of the lower fidelity solver for use in conjunction with the higher fidelity solver. In the first optimization cycle, the target $C_{L\max}$ is not known in advance; therefore, when solving the inverse problem, we set C_L near $C_{L\max}$ of original airfoil. The original airfoil is N230m airfoil, which was obtained in the previous paragraph from the NACA23012 airfoil by modifying its lower surface to increase the value of the pitching moment. In this case, the target distributions of the pressure coefficient are obtained from the distribution of the pressure coefficient obtained from the solution of the direct problem at C_L = 1.4 with subsequent modification in the vicinity of the nose peak at $s_{11} < < s_{21}$.

Figure 4 shows the original (N230m) and optimal (from the point of view of two different solvers) distributions of the pressure coefficient in the vicinity of the peak, depending on the arc length, obtained from the inverse problem solution during optimization.

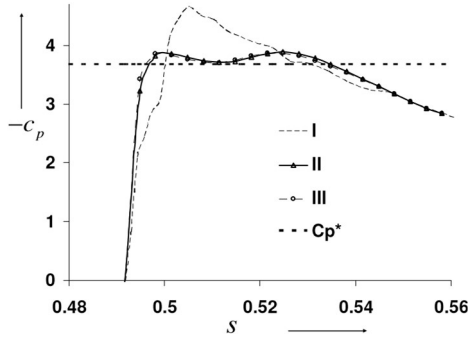

Figure 4: I- original (N230m) airfoil, optimal airfoils (airfoil 2): II - CFD, III – VIS. M_∞ =0.4, C_L =1.4

As expected, the optimal distributions in the correction range are close to C_{p^*} level. On the next figures, the data for the optimal airfoils obtained on the basis of solvers of different fidelity levels are indicated by Roman numerals: II - CFD solver, III - VISTRAN solver. For better clarity, discrete data is connected with lines.

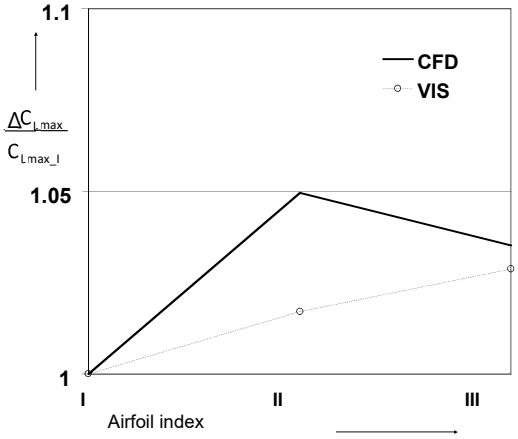

Figure 5: I- original (N230m) airfoil, optimal airfoils (Airfoil 2): II - CFD, III – VIS

Figure 5 shows a graph-diagram, which compares the values of $\frac{\Delta C^{Lmax}}{C_{Lmax\_I}}$, the relative increase in the maximum lift of the optimal (from the point of view of different solvers) airfoils, calculated by different solvers in comparison with the original airfoil. Results obtained using VISTRAN solver do not match quantitatively or qualitatively with the high fidelity solver result. However, the CFD calculation shows that both solvers allow following correctly the direction of the search for the optimum and therefore can be used to speed up the optimization procedure.

The relative increase in the lift coefficient was: 5% - airfoil II (CFD), 3.5% - airfoil III (VIS), which can be considered as a significant result of aerodynamic design. Slightly ahead of events, it should be noted that in reality even greater growth was achieved, Figure 6, but in order to obtain it, the $K_{\max}$ value constraint was weakened. In this case both solvers give the same result

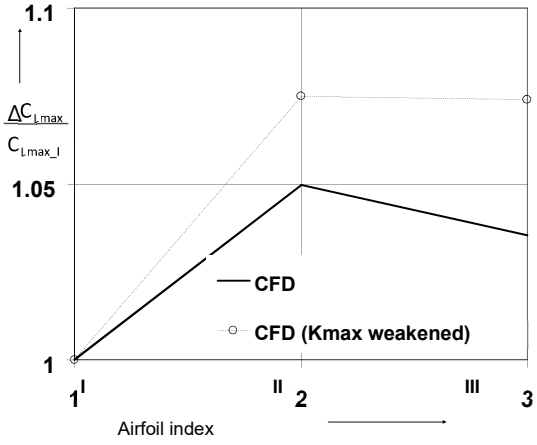

Presented at 46th European Rotorcraft Forum, Moscow, Russia, 9-11 September, 2020

Figure 6: I – original airfoil, optimal airfoils: II - CFD, III - VIS

The results obtained at the first optimization cycle confirm that the new method allows increasing maximum lift of the airfoil at a given value of the pitching moment coefficient at zero lift.

It is known that, for helicopter-type airfoils $K_{\max}$ value is achieved at 0.6<C_L <0.7, therefore, at the second stage of the optimization process, when solving the inverse problem, for definiteness, we set C_L = 0.65.

The target distributions of the pressure coefficient are obtained from the distributions of the pressure coefficient obtained from the solutions of direct problems for airfoil 2 (NACA230m+) with subsequent modification in the interval $s_{12} < s < s_{22}$. The $C_{L\max}$ values achieved during the first optimization cycle (different for different solvers) are set as constraints, along with constraints on C_{d00} near M_{dd} value.

Figure 7 shows the original, (airfoil 2) and optimal (from the point of view of different solvers) distributions of the pressure coefficient in the correction zone, depending on the arc length, obtained from the GIP solution when optimizing the $K_{\max}$ value. As expected, optimal distributions allows establishing the correction range leading to a weakening of the shock wave (in this case, to its practical disappearance).

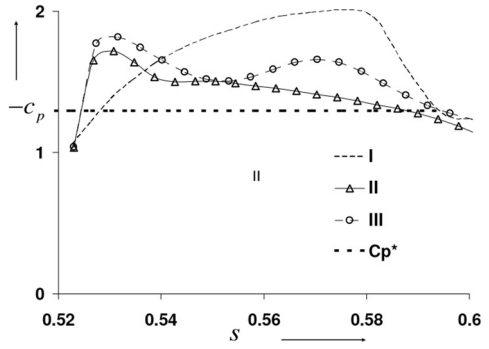

Figure 7:I- original (airfoil 2) airfoil, optimal airfoils (airfoil 3): II - CFD, III – VIS, M_∞ =0.6, C_L =0.65

.

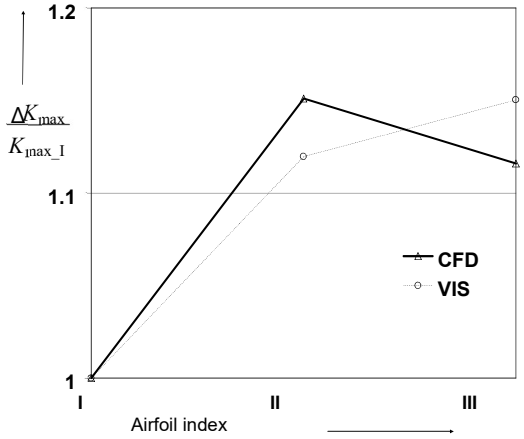

Figure 8: I- original (airfoil 2) airfoil, optimal airfoils (airfoil 3): II - CFD, III – VIS

Figure 8 shows a graph-diagram that compares the values of the relative gain of the maximum aerodynamic efficiency $\frac{\Delta K^{\max}}{K_{\max\_I}}$ of the optimal (from the point of view of different solvers) airfoils, calculated by different solvers, and the original airfoil. Again the results obtained using VISTRAN solver does not match quantitatively or qualitatively with the high fidelity solver result. However, the CFD calculation shows that both solvers allow following correctly the direction of the search for the optimum and therefore can be used to speed up the

The increase in the lift coefficient was: 15% - airfoil III (CFD), 12% - airfoil IV (VIS), which can be considered as a significant result of aerodynamic design.

At the third step, when solving the inverse problems, as the initial distribution of the pressure coefficient, we use the distribution obtained from solving direct problems at $M_\infty < M_{dd}$ for the airfoils obtained at the second step. The target distributions of the pressure coefficient are obtained by modifying the initial distributions in the interval $s_{13} < s < s_{23}$ in order to weaken the shock waves at the conditions near M_{dd}.

Figure 9 shows the airfoils contours and performances calculated by the CFD RANS solver. The calculations confirm the effectiveness of the proposed procedure for aerodynamic design, which is based on physical considerations that allow improving the main performances by properly adjusting the pressure coefficient distributions. The figure shows that generally with three optimization cycles, it was possible to significantly improve all three main integral criteria with holding pitching moment value at zero lift.

Presented at 46th European Rotorcraft Forum, Moscow, Russia, 9-11 September, 2020

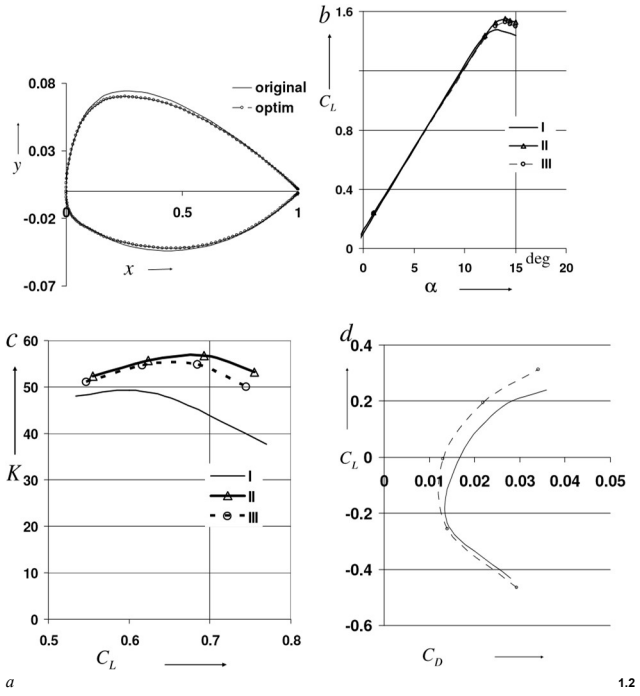

Figure 9: a- airfoils contours; b- $C_L(\ )\alpha$, M_∞ =0.4;

c- $C_L/C_D(C_L)$, M_∞ =0.6; d- $C_L(C_D)$, M_∞ =0.8

The combined method is, of course, a local optimization method. It allows to vary the main airfoil performances with the changing the geometry in a small neighborhood of the original profile. In contrast to the direct optimization method, it uses the design variables based on physical considerations. This allows adopting the optimization process in the direction necessary for the user and significantly reduces the number of iterations required to achieve the optimum.

CONCLUSION

The application is given of the concept of the GIP for helicopter airfoil design. The improving variations of pressure distributions for NACA series airfoil are considered: the increase of the zero lift pitching moment without noticeable loss of airfoil maximum lift and lift to drag ratio at middle Mach number; the increase of airfoil maximum lift at low Mach number without noticeable changing of other

integral criteria;
the increase of lift to drag ratio at middle Mach number without noticeable changing other integral criteria;
the interactive decrease of wave drag at high Mach number without noticeable changing other integral criteria.

Thus it was established that mathematical model based on the concept of GIP and simple physical considerations allows modifying pressure distributions successively for improving helicopter airfoils performances.

Instead of a set of blade sections geometry parameters [5-11] may be considered section local C_p design parameters that allow changing a vector of aerodynamic performance in needed direction based on physical considerations. In preliminary blade design stage the geometry of blade sections may be corrected with some dozens iterations. The technique considered is suitable for design using solvers of any fidelity.

References

[1] Bauer F., Garabedian P., Korn D. Supercritical wing sections III. // Lecture Notes in Economics and Math. Syst., 1977, N 150.

[2] Nikolsky A.A. Generalized inverse airfoil problem. Tsagi Science Journal, vol. 43, i. 6, 2012, pp. 775-786.

[3] Lyapunov S.V. , A.V.Wolkov. Numerical Prediction of Transonic Viscous Separated Flow Past an Airfoil // Theoretical and Computational Fluid Dynamics. –1994. –V.6, N 1, P.49-63.

[4] Morrison J. H. A Compressible Navier-Stokes Solver with Two-Equation and Reynolds Stress Turbulence Closure Models// NASA CR-4440, May 1992.

[5] Sobieczky, H.. Parametric Airfoils and Wings, "Notes on Numerical Fluid Mechanics ,Vieweg Verlag, Vol. 68, pp.71-88, 1998.

[6] Robinson, GM, and Keane. AJ, Concise Orthogonal Representation of Supercritical Airfoils. Journal of Aircraft, Vol. 38, No. 3, pp. 580-583, 2001.

[7] Padula, S., and Li, W., Options for Robust Airfoil Optimization Under Uncertainty. 9th AIAA Multidisciplinary Analysis and Optimization Symposium, paper No. 2002-5602, pp.1-7, 2002.

[8] Song, W., and Keane, AJ, A Study of Shape Parameterization Airfoil Optimization. AIAA-20044482, 10th AIAA / ISSMO Multidisciplinary Analysis and Optimization Conference, pp.1-8, 2004.

[9] Samareh, JA. Aerodynamic Shape Optimization Based on Free-Form Deformation. AIAA 2004-4630, pp.1-6, 2004.

[10] B. M. Kulfan. Recent extensions and applications of the 'CST' universal parametric geometry representation method. The Aeronautical Journal, 2010, vol. 114, no. 1153, pp. 157-176. [11] Nikolsky A.A. Universal geometric transformation method PGT for aircraft

Presented at 46th European Rotorcraft Forum, Moscow, Russia, 9-11 September, 2020

design // 46-th European rotorcraft forum. -2018. –V. 1. –N 40. – pp. 456-467.

Presented at 46th European Rotorcraft Forum, Moscow, Russia, 9-11 September, 2020